NIFS--200

JP9304158

# Roles of Electric Field on Toroidal Magnetic Confinement

K. Itoh, S.-I. Itoh, H. Sanuki and A. Fukuyama

(Received – Nov. 4, 1992)

NIFS-200 Nov. 1992

# Roles of Electric Field on Toroidal Magnetic Confinement

Kimitaka Itoh*, Sanae-I. Itoh†, Heiji Sanuki*
and Atsushi Fukuyama††

* National Institute for Fusion Science, Nagoya 464-01, Japan
† Research Institute for Applied Mechanics, Kyushu University 87, Kasuga 816, Japan
†† Faculty of Engineering, Okayama University, Okayama 700, Japan

**Abstract**

Theoretical research on the influence of the electric field on the toroidal magnetic confinement is surveyed. The static electric field is first described. Physics pictures on the generation of the radial electric field and the influence on the confinement are shown. Neoclassical effects as well as the non-classical processes are discussed. Emphasis is made on the connection with the improved confinement. Convective cell, i.e. the nonuniform potential on the magnetic surface is also discussed. The roles of the fluctuating electric field are then reviewed. The progress in the recent theories on the anomalous transport is addressed. Through these surveys, the impact of the experiments using the heavy ion beam probes on the modern plasma physics is illustrated.

Keywords: Electric Field, Plasma Confinement, Toroidal Plasma, Fluctuations, Anomalous Transport, Inward Pinch, L-mode, H-Mode, Improved Confinement, Transition, Plasma Flow, Loss Cone

## Contents

## §1. Introduction

Toroidal plasma confinement is the research to *confine the* high temperature plasma in toroidal magnetic confinement. The studies on the toroidal plasma equilibrium and magnetohydrodynamic (*MHD*) stability *have been the* main subject in this field of plasma physics. It has been well known, however, from the beginning of the experimental research in the plasma confinement, that the plasma loss process is much faster than the expectation which is based on the binary collision of charged particles. This has been known as the anomalous transport[1]. The majority of the modern plasma physics related with the fusion research has aimed the resolution of the anomalous transport processes. In understanding the plasma loss processes, *the electric field is* considered to have the key role for the plasma confinement.

The electric field can influence the confinement in two ways. *First, the static structure of it takes an* important part of the concept of the confinement. The intrinsic importance of the electric field on the plasma confinement through E×B rotation [2] was discussed much in the bumpy torus configurations [3]. In this configuration, the E×B drift has the essential role for the plasma confinement. The progress in the research has revealed that the electric field has important roles in stellarators[4-6] as well; very recently, it is recognized that the radial electric field plays essential roles even in tokamaks[7-9]. This finding has urged the recent flourishing in studies on the electric field in toroidal devices.

The second aspect of the influence of the electric field is the fluctuations[1,10-12]. The electric fluctuations has long been the candidate of the origin of the anomalous transport. Theories have discussed lot of instabilities and associated fluctuations, trying to identify the cause of the cross field transport. The recent progress in experimental observation has enabled the direct comparison between fluctuations and transport [13], thus providing the confirmation that the electric field fluctuation plays essential role on the anomalous transport. The method of the heavy ion beam probes has shown the inevitable contribution in the research on these two aspects of the plasma confinement[14].

In this article, we review the theoretical studies on the static electric field structure and the fluctuating electric field in toroidal plasmas, making the emphasis on the recent progresses. We try to illustrate the generic nature of toroidal plasmas by choosing the topics from studies on tokamaks and stellarators. Through these reviews, we intend to clearly show how the measurement on the various aspects of the electric field has the essential importance in the modern plasma physics as well as in the fusion research. For this purpose, the example in this article may be limited, and the references are not exhaustive. Though the parallel electric field (the electric field which is parallel to the main magnetic field) has important influences on the confinement [15,16], it is out of the scope of this survey. Other important omission is the influence on the behaviors of the impurities.

## §2. Static Structure of the Electric Field

In this section, we consider the structure of the global electric field. The theoretical model to describe the generation of the radial electric field is first surveyed. The impact on the confinement is *next explained in connection* with the improved confinement such as the H-mode and the peaked density profile. The dynamic response is also discussed. Brief comment is made on the variation of the potential on the magnetic surface.

### (2.1) Generation of the Global Electric Field

The radial electric field solution in the steady state is evaluated by the ambipolarity equation

$$\Gamma_i = \Gamma_e, \tag{1}$$

where $\Gamma$ is the radial particle flux and suffix e and i denote electrons and ions, respectively. Taking into account nonclassical terms, we write $\Gamma_i$ and $\Gamma_e$ as

$$\Gamma_i = \Gamma_i^{NC(s)} + \Gamma_i^{NC(as)} + \Gamma_i^{orbit} + \Gamma_{fcx} + \Gamma_{icx} + \Gamma_{i,a}, \tag{2}$$

$$\Gamma_e = \Gamma_e^{NC(s)} + \Gamma_e^{NC(as)} + \Gamma_{e,a}. \tag{3}$$

These equations consist of the neoclassical fluxes (denoted by the superscript of NC), the direct ion orbit loss flux ($\Gamma_i^{orbit}$), the charge exchange contributions of fast ions ($\Gamma_{fcx}$) and bulk ions ($\Gamma_{icx}$), and that driven by the anomalous transport ($\Gamma_a$). The orbit loss and cx loss of electrons are not taken into account, because the electron mass is much smaller than that of ions.

The neoclassical contribution is given as the sum of the flux $\Gamma_i^{NC(s)}$, associated with the passing and toroidally trapped particles, and $\Gamma_i^{NC(as)}$ related to the ripple trapped particles, as is reviewed in Ref.[4].

The explicit form of the ion orbit loss is discussed in literatures. It follows, for tokamaks, that[7,17]

$$\Gamma_i^{orbit} \simeq \rho_p n_i \nu_i \varepsilon^{-0.5} \exp(-\Xi X^2) \qquad (4)$$

where $\nu_i$ is the ion collision frequency, $\varepsilon = a/R$, $\Xi$ indicates the effect of orbit squeezing due to the inhomogeneity of $E_r$[18], and $X = eE_r\rho_p/T$. ($X$ is equal to the poloidal Mach number $V_pB/v_{Ti}B_p$ if $V_p = E_r/B_t$.)

In the case that the direct loss of fast ions has the largest contribution, such as the case of stellarators, we have a simple expression as[19]

$$\Gamma_i^{orbit}(r) \simeq [P(r) - P(r_*)]/4\pi^2 rRW_b \qquad (5)$$

where P(r) is the input power crossing through the minor radius r, $W_b$ denotes the beam energy, and $r_*$ is the radius representing the loss boundary. The dependence of the radius $r_*$ on the radial electric field, $r_*[E_r]$, was discussed and the expression is given in Ref.[20].

The fast particle flux is also generated by the charge exchange loss. The charge exchange process conserves a local charge, but takes away the momentum. This loss of momentum causes the drift flux in the radial direction. Simplifying that the fast particle velocity is characterized by the toroidal one, $v_f$, we have

$$\Gamma_{fcx} \simeq (M_f n_f n_0/eB_p)\langle\sigma_{cx}v\rangle v_f, \tag{6}$$

where $M_f$ is the fast ion mass, $n_f(r)$ is the fast ion density, and $n_0(r)$ is the neutral particle density.

The charge exchange of bulk ions with neutrals can cause the radial electric field [21]. In tokamaks, the toroidal force balance is used [22], because the bulk ion viscosity directs in the poloidal direction [23]. The flux is given as

$$\Gamma_{i,cx} = (qR/ZerB)n_i m_i U_\phi n_0\langle\sigma_{cx}v\rangle, \tag{7}$$

where the toroidal rotation is given by

$$U_\phi = (qT_iR/ZerB)[n_i'/n_i(1+c_i\eta_i) - ZeE_r/T_i] + qRU_p/r, \tag{8}$$

where $\eta$ =dlnT/dlnn, and $c_i$ is a numeric.

In helical systems, the toroidal rotation damps off due to the large helical ripple and the poloidal flow remains[23]. The main ions are rotating mainly in the poloidal direction. The induced radial flux by this poloidal force is

$$\Gamma_{icx} = (Mn_i n_0 T_i/e^2B^2)\langle\sigma_{cx}\rangle[ZeE_r/T_i - \{1+\eta_i(\mu_{i1}/\mu_{i2})\}n_i'/n_i] \quad (9)$$

where M is the ion mass, and $\mu_{i1}$ and $\mu_{i2}$ are neoclassical viscosity coefficient.

The radial electric field solution in the steady state is evaluated by the ambipolarity equation (1). Through the dependences of $\Gamma$ on $E_r$, the ambipolarity equation, Eq.(1), is a nonlinear algebraic equation with respect to the radial electric field. Equation (1) can have multiple solutions on each magnetic surface, which is discussed in §2.2. We look for the solution which is continuous and satisfies the condition

$$E_r(r) \to 0 \text{ as } r \to 0. \quad (10)$$

Lot of work have been done on the analysis of Eqs(1)-(10). An example of the solutions is shown in Fig.1 for the case of stellarators. Eq.(1) is solved with the experimentally obtained plasma profiles in CHS [24]. Figure 1(a) illustrates the prediction of the radial electric field. The dotted line indicates the neoclassical estimates. The correction by the direct orbit loss of ions are taken into account for the solid line. The dashed line indicates the result where the cx loss effect is added. Figure 1(a) shows that the fast ion losses, which are caused by the loss cone and cx with neutrals, are always positive and make the electric field more negative.

The boundary of the loss cone is also determined selfconsistently by solving Eqs.(1)-(10). Figure 1(b) shows the loss cone boundary in the low field side. The solid line indicates the self-consistent solution, while the dashed line is the result in which the parabolic approximation is made. It is noted that the influence of the orbit loss on $E_r$ appears only in the region $r > 0.8a$, although the loss cone boundary is given by $r > r_*$ and $r_* \simeq 0.3a$.

## (2.2) Influence on the Confinement

Recently various improved modes have been found. In the H-mode plasmas [25,26], the steep gradient is established only near the edge. Other improved modes are characterized by peaked density/ion temperature profiles[27,28]. We present a model of improved confinement based on the influence of the radial electric field on the core confinement.

## Model of Inward Pinch and Peaked Profile Modes

The inward particle pinch has been one of the mysteries in the toroidal confinement. The neoclassical theory has shown that the neoclassical viscosity can induce the particle flux in the presence of the toroidal electric field. This is known as the Ware pinch[15]. Experiments reported that this neoclassical theory explains some of the observations. However, the inward pinch of particles in experiments has shown much varieties, and cannot be fully explained by the Ware pinch: The impressive example is found in the case of the peaked density profile in the improved confinement such as the improved Ohmic confinement (IOC). We here explain theoretical studies to understand this phenomena, where the role of electric field is predicted to be essential [29].

Density continuity and charge conservation in the presence of the diffusion determine the structure of $E_r(r)$ and density profile $n(r)$. To obtain $E_r(r)$ in the presence of the diffusion, the electron and ion fluxes are assumed to be anomalous due to drift-type microturbulence of frequency, $\omega$, and poloidal wave number, $m$. Applying quasilinear theory, $\Gamma_a$ is given in Refs.[30,31]. The ion flux includes an anomalous viscosity flow,

$$\Gamma_{i,v}=(qR/ZerB)n_i m_i \nabla\mu_\perp \nabla U_\phi, \qquad (11)$$

($\mu_\perp$: viscosity)[32]. The continuity equation $\nabla\cdot\Gamma_{e,i,tot}=S_{e,i}$ closes the basic equations. The bipolar contribution of the neoclassical flux and direct orbit loss are neglected here, which are important for the phenomena near the edge and are discussed in the next subsection.

The particle sources, $S_{e,i}$, and $\Gamma_{i,cx}$, are localized near the edge and $S_e = S_i$ ($S \equiv n_0 n_e \langle\sigma_i v\rangle$; where $\langle\sigma_i v\rangle$ is the ionization rate). The normalized electric filed, $\mathbf{E}$ ($=a^2 eE_r/rT_i$), and its shear part $\{E\}$($\equiv\mathbf{E}$-const) are used. Simplifications are introduced as $\eta=0$ with $T_e = T_i$ and $U_p \to 0$. $D$, $\mu_i$ and $q$ are set to be numeric. In the core, where $n_0 \sim 0$, $\Gamma_{e,tot} = 0$ gives the relation $-2(\ln n)' = \{E\} + C_l$ in $y$ ($=r^2/a^2$) coordinate. $C_l$ ($\propto \langle\omega/m\rangle$, $\langle\omega r/m\rangle$ is spectrum averaged phase velocity,) is assumed to be constant, which is determined by boundary conditions. For the boundary condition at $r=a$, $(dn/dr)_{r=a} = n/\lambda_n$, Eq.(1) gives

$$\{E\} = \{\left(\frac{a}{\lambda_n} - \frac{a^2}{2D_e}\langle S\rangle_{r=a} - C_l\right) \frac{I_0(\sqrt{\nu_a/\nu_\mu}\, r^2/a^2)}{I_0(\sqrt{\nu_a/\nu_\mu})}\} \tag{12}$$

in the limit of $\Delta << a$ ($\Delta$: penetration length of neutrals) where $\langle S\rangle = \int n_e n_0 \langle\sigma_i v\rangle dy / n_e y$, where $\nu_\mu = (1/Z+1) q^2 R^2 \mu_i / a^4$, $\nu_a = (1+Z) D_i / \rho_i^2$ and $\rho_i$ is the ion gyroradius.

Figure 2 shows the density profile n(r) for various values of $\nu_\mu/\nu_a$ and a fixed line averaged density. The profile of $E_r$ is dictated by the parameter $\nu_\mu/\nu_\alpha$, which indicates the diffusion Prandtl number[33]. The more viscous plasma has the more peaked profile. Viscous frictional force to the toroidal rotation and the poloidal magnetic field causes the FxB drift of ions. Only if the rotation flow is counter to the current direction the inward drift occurs. The reduction of the edge neutrals leads to the peaked profile. The peaked profile can be thus sustained without particle source at the core. Associated with the density peaking, the rotation profile also peaks. The SOC/IOC transition[27] is attributed to this mechanism[29].

## Physics Picture of H-Mode

*One of the most dramatic findings in recent plasma confine*ment experiments was the H-mode[25,26]. It has shown the generic nature of the edge plasma, i.e., that the multiple states are allowed *for given external conditions*, that typical gradient lengths can be disconnected from the minor radius, and that the transition has a rapid time scale. A possible mechanism of the *multiple state of confinement* was proposed by taking into account the effect of the radial electric field. The field can be multi valued by the loss cone[7]. The basic physics picture is as *follows. The gradient-flux relation* should be multi-valued to explain the sequence of the transition; this relation should have the form, which is schematically drawn in Fig.3. This multi-*valued form is possible* at edge (*not* characterized by the separatrix).

The stationary solution is obtained by solving Eq.(1). Figure 4(a) illustrates the case study that the bipolar part of the anomalous flux,

$$\Gamma_{a,e} - \Gamma_{a,i} \propto (-n'/n + eE_r/T_e). \qquad (13)$$

The jump of $\Gamma$ is predicted, by balancing the ion orbit loss $\Gamma_i^{orbit}$ with $\Gamma_{a,e}-\Gamma_{a,i}$ in Eq.(1), at the critical gradient

$$\lambda = \rho_p n'/n = \lambda_c, \quad \text{and } \lambda_c \sim O(1) \qquad (14)$$

as is shown in Fig.4(b). This example shows that the singularity of the transport property $\Gamma[\nabla n]$ can be explained by using a <u>continuous</u> function of $\Gamma[E_r]$. *An extension of the model is* possible by considering the bulk viscosity contribution in $\Gamma_i^{NC}$[17]. The bulk viscosity generates the force on ions in the poloidal *direction as*

$$F_p \sim -m_i n_i \nu_i q^2 V_p f(X). \tag{15}$$

and

$$\Gamma_i^{NC(s)} = F_p/eB. \tag{16}$$

The function $f(X)$ is unity for $|X|<<1$ and *behaves like* $exp(-X^2)$ (plateau regime) or $X^{-2}$ (Pfirsch-Schluter regime)[17,23]. Figure 4(c) illustrates the balance of $\Gamma_i^{orbit} = -\Gamma_i^{NC(s)}$, confirming that the bifurcation can *occur* at a particular value of the edge gradient, $\lambda_c \sim O(1)$. A variety of bifurcations is predicted. When the electron term $\Gamma_e$ is negligible, the transition occurs *for* a more negative $E_r$, and that for a more positive $E_r$ takes place if $\Gamma_e$ is important. This latter case occurs in the case of energetic electrons (such as the lower hybrid wave heating), in which $\Gamma_e^{NC(as)}$ is effective [34].

The proposal of an electric bifurcation[7] was tested by experiments. D-III D[8] and JFT-2M[9] confirmed the existence of a radial electric field. The transition can be excited by a radial current driven by the probe and by an external circuit[35]. *The layer width is of the order of* $\rho_p$[9]. (They do not coincide. The relation between them is discussed in the next subsection.) The nonlinear response of $F_p$ to X is confirmed by the biasing experiment[36]. Influence of the energetic electrons has also been seen on JT-60 [37].

## (2.3) Dynamics in the Transition

The dynamics associated with the *transition* must be studied in order to perform the complete comparison with experiments. To quantify the model, it is necessary to study the nature of the viscosity term in the basic equation. We write the Poisson equation combined with the equation of motion as

$$\varepsilon_0 \varepsilon_{\perp} \partial E_r / \partial t = e(\Gamma_e - \Gamma_i) \qquad (17)$$

where $\varepsilon_{\perp}$ is the perpendicular dielectric constant. RHS of Eq.(17) vanishes in assuming that the stress tensor $\Pi$ to be the diagonal.

Various types of edge localised modes (ELMs) are known in experiments[38]. Some is correlated with the critical gradient of edge pressure against the ballooning mode[39], and some is not. The bifurcation theory provides a model for small and continuous ELMs[40]. Hysteresis between $\nabla n$ and $\Gamma$ can generate an oscillation ('limit cycle solution'). The dynamical equation (17) is solved together with the continuity equation and the model equation $\Gamma[X, \nabla n]$. A model equation can be formulated in the form of the Ginzburg-Landau equation as [40]

$$\partial n/\partial t = (\partial/\partial x)D(X)\partial n/\partial x, \tag{18-1}$$

$$\nu\partial X/\partial t = -N(X,\lambda,n) + \mu\partial^2 X/\partial x^2 \tag{18-2}$$

where D is an effective diffusivity, $x=a-r$, $\nu$ is a smallness parameter of the order of $(\rho_i/\rho_p)^2$, $\mu$ is the shear viscosity, and $N$ represents the current $e[\Gamma_i^{orbit}+\Gamma_i^{NC(s)}-\Gamma_e]$ which contains the nonlinearity and depends on both $E_r$ and $\nabla n$. Introduction of the shear viscosity allows us to study the radial structure of the barrier. (Note that normalization is used as $x/\rho_p\to x$, $D/D_0\to D$, $\mu/D_0\to\mu$, $t/(\rho_p^2/D_0)\to t$, and $D_0$ being the diffusivity in L-phase.)

A simplified model was studied where $N(X,\lambda,n)$ is given $N(X,g)$ ($g\equiv\lambda/\nu_i$) and $N(X,g)$ is modelled by the cubic equation as in Fig.5(a). It is shown that the set of equations (18) predicts the self-sustaining oscillation for a fixed value of the flux from the core plasma. This oscillation is possible in a limited area of the parameter space. Otherwise, either the high-confinement state (H) or low confinement state (L) is allowed. Figure 5(b) and (c) illustrate the oscillatory solution of the out-flux, and the radial profile of the effective diffusivity in H and L phases. In the phase of good confinement, the reduction of D extends from the surface to the layer, the characteristic width of which is given by $\sqrt{\mu/D}\rho_p$.

The result of the layer width illustrates the importance of the viscosity on the radial electric field structure. It is also noted that the layer width is not necessarily equals to the poloidal gyroradius, as is shown in Fig.1.

### (2.4) Convective Cell

The electric potential is not necessarily constant on the magnetic surface: In this case, the poloidal electric field is generated and the E×B convection causes the plasma flux across the magnetic surfaces. This phenomena is known as the convective cell. Since the potential inhomogeneity must be sustained against the parallel conduction of electrons, this phenomena is characteristic to the cold plasma and to the strongly-localized heating/cooling. Hence they are commonly observed near the plasma edge. As is discussed in §2.2, the edge plasma has strong influence on the core confinement, and this phenomena also needs careful studies.

Global instabilities such as MARFE[38] and detachment are known. The energy loss by the line radiation by light impurities increases as the electron temperature decreases. Thus the radiation loss can cause the thermal instability. The radiation loss is modelled as $S_E = -n_e n_I L(T_e)$, where $n_I$ is the impurity density. Models on $L(T_e)$ and the dynamic response of $n_I$ with respect to the perturbation are necessary to quantify the growth rate. The latter is usually denoted by the parameter $\xi = -(\tilde{n}_e/n_e + \tilde{n}_I/n_I)(T/\tilde{T})$. Asymmetric thermal instability ($m=1/n=0$, i.e., MARFE) can grow if[41]

$$n_I[\partial L/\partial T + \xi L/T] > (\chi_\perp/(a-r_b)^2 + \chi_\parallel/q^2R^2), \qquad (18\text{-}1)$$

and

$$\xi n_I L/T > \chi_{\parallel}/q^2 R^2, \tag{19-2}$$

hold, where $[r_b, a]$ is the range of the analysis, where $\partial L/\partial T$ is negative and large. The inhomogeneity of the temperature along the field line, $\tilde{T}$, is associated with the thermal electric field. The region of the strong radiation of MARFE is negatively charged.

If the condition Eq.(19-2) does not hold, the poloidally symmetric mode (i.e., detachment) starts to grow. This picture is often referred to as an origin of the "density limit". The lighter impurities (for which $\partial L/\partial T<0$ for the lower plasma temperature) leads to a MARFE, while the heavier one to detachment (and then to disruption): These predictions are consistent with experiments.

## §3. Fluctuation and Anomalous Transport

The other and important aspect of the influence of the electric field on magnetic confinement is the fluctuation-driven transport. In this section, we survey some of recent progresses in the analysis of the transport process by the electric fluctuations.

### *(3.1) Electric Fluctuation and Anomalous Transport*

The physics picture of the fluctuation-driven transport has been reviewed in literatures (see for instance Ref.[1,10]). The local coordinates is taken as in Fig.6 for the inhomogeneous plasma. In the presence of the electric field in the y-direction ($\nabla n \times B$ direction), the plasma is subject to the E×B motion in the x-direction (i.e., density gradient). The step size of the excursion is given as $\delta = E_y/\omega B$ ($\omega$ being the oscillation frequency). When the fluctuation is generated and decays with the characteristic time of $\tau_c = 1/\gamma$, the random walk with the step size of $\delta$ causes the diffusion of the order of $D = \gamma\delta^2$. The level of the fluctuation is also estimated. The fluctuations can grow until the local gradient shows the flattening. This leads to the estimate of $\tilde{n}/n \sim e\tilde{\Phi}/T \sim 1/k_x L_n$, where the symbol ~ indicates the fluctuation component and $L_n$ is the density gradient scale length. Except a numerical coefficient of the order of unity, D is expressed as[1]

$$D \simeq \tau / k_x^{\,2}. \tag{20}$$

This expression is called the mixing length estimate of the turbulent transport. More detailed nonlinear treatment has confirmed, at least qualitatively, these physics considerations [42,43].

As is shown in the following, the decorrelation rate $\tau$ and typical scale length $1/k_x$ are dependent on the plasma parameters. *This explains one characteristic point of the plasma transport,* that the plasma structure itself influences the transport coefficients.

The other feature of the plasma is the interference between *the fluxes of* the mass, momentum and heat. The magnetic confinement plasmas are usually sustained by the energy source near the axis. The injection of the energy (such as OH, NBI or RF heating) leads to the peaked density profile or generates the plasma rotation. (The example of the analysis is shown in §2.) The relation between the fluxes and thermal forces are given, using the transport matrix $\mathbf{M}$, as [32,44]

$$\begin{pmatrix} \Gamma_e \\ J_\phi / e \\ q_e / T_e \end{pmatrix} = \mathbf{M}_e \begin{pmatrix} X_{1e} \\ eE_\phi / T_e \\ -T_e' / T_e \end{pmatrix} \tag{21}$$

and

$$\begin{pmatrix} \Gamma_i \\ P_{\phi r}/m_i v_{Ti} \\ q_i/T_i \end{pmatrix} = M_i \begin{pmatrix} X_{1i} \\ -2V_\phi'/v_{Ti} \\ -T_i'/T_i \end{pmatrix} \qquad (22)$$

where $\Gamma$ and $q$ are the particle and heat fluxes, $J_\phi$, $V_\phi$ and $E_\phi$ are the current, velocity and electric field in the toroidal direction, respectively, $P_{\phi r}$ is the radial flux of the toroidal momentum, ' denotes the derivative with respect to the minor radius $r$, $v_T$ is the thermal velocity, and the thermodynamical force $X_1$ is defined as

$$X_1 = -n'/n + e_\pm E_r/T + T'/2T - e_\pm B\omega/k_\theta T. \qquad (23)$$

In this expression, $e_\pm$=e for ions and -e for electrons.

These relations between fluxes and gradients govern the mixing in the transport processes. The impact on the density profile is discussed in §2. That for the heat transport is also derived. If one studies the confinement near the core, the energy transport is often dominated by the conduction. The density gradient (and velocity gradient as well) is sustained not by the particle source but by the off diagonal term in Eqs.(21) and (22). In such a case, the limit of $\Gamma\simeq0$ is used to yield[32]

$$q_i = -[M_{33} - M_{13}^2/M_{11}]\ T_i'/T_i. \qquad (24)$$

The ratio between the heat flux and the temperature gradient is often referred to as the effective thermal conductivity. This result indicates that the effective thermal conductivity is not the 33 component of the transport matrix but is influenced by the off-diagonal elements. [Owing to the Shwartz inequality the term in the brackets [] in Eq.(24) is positive definite. However, the absolute value can be smaller than $M_{33}$.]

Application of the theories to hot plasmas has been done focusing on the drift waves. The tokamak configuration has the averaged magnetic well. However, for the particles which are trapped in the bad curvature region due to the toroidal field inhomogeneity, the time-averaged curvature is unfavorable. The diamagnetic drift direction of the trapped particles coincides with that of the curvature drift, and the trapped particles can destabilize the drift waves. The typical level of the growth rate is calculated to give the transport coefficient

$$D = C \sqrt{\frac{r}{R}} \frac{\rho_i}{L_n} \frac{T_e}{eB} \tag{25}$$

where C is a numerical coefficient of the order of unity. Recent transport theories based on the drift wave is given, for instance, in [43].

L mode confinement has been observed in all tokamaks, where the energy confinement time decreases as the plasma temperature (or the heating power) is increased [45,46]. Microscopic fluctuations have been confirmed to play an important role in anomalous transport[13]. The outcome of the theories on the low frequency fluctuations is compared to the experimental results. The characteristics of the L-mode confinement is the power degradation of $\tau_E$. This phenomena may be modelled by the relation $\chi \sim T^{1.5}/aB^2$, which has been derived for drift wave theories, Eq.(25). However, this form of $\chi$ contradicts to the radial form of $\chi$, i.e., $\chi$ increases towards the edge in experiments, where the temperature is low. These facts require the basic reconsideration on the theory of the anomalous transport based on the microscopic fluctuations.

Ohkawa's model, $\chi \sim \delta^2 v_A/qR$ ($\delta$ is the collisionless skin depth, $R$ the major radius, $q$ the safety factor and $v_A$ the Alfven velocity), is one of the few models explaining that $\chi$ is large at high temperature and becomes larger towards the edge, as well[47]; it could not, however, fully explain the dependences of $\tau_E$. The very recent progress, which may resolve these difficulties, is discussed in the next subsection.

## (3.2) Model of Turbulence

We here explain the recent progress on the theory of the self-sustaining turbulence. The importance of the self-sustaining turbulence has been recognized[45-47], and the analysis on the pressure-gradient driven turbulence has recently shown a break through. The plasma transport process, in one hand, enhances the mode growth through the current diffusivity (i.e., the electron viscosity), while at the same time stabilize the mode through the thermal conductivity and ion viscosity. The mode growth leads to the enhancement of the transport coefficients. The self-sustained state is determined by the balance between the mode amplitude and transport coefficients. In the following, we describe the recent achievement in the theoretical clarification on the self-sustained turbulence and anomalous transport [50].

We analyse the circular tokamak and use the reduced set of equations and keep the current diffusivity term in Ohm's law,

$$E+v\times B=J/\sigma-\nabla^2\lambda J, \tag{26}$$

where $\sigma$ is the conductivity and $\lambda$ is the current diffusivity [51]. The ballooning transformation is applied, and it is found that the current diffusivity, not the resistivity is the main mechanism to destabilize the pressure driven instabilities which are relevant for the anomalous transport process. The growth rate of the short wave-length mode, driven by the $\hat{\lambda}$ term, is given analytically by $\hat{\gamma} \simeq \hat{\lambda}^{1/5}(nq)^{4/5}\alpha^{3/5}s^{-2/5}$. [Notations are: $\gamma$ is the growth rate, $\alpha=q^2\beta'/\varepsilon$, $\varepsilon=a/R$, $s=rq'/q$, $\beta$ is the pressure divided by the magnetic pressure, and $'$ denotes the derivative with respect to r/a. We use the normalizations: $r/a\to r$, $t/\tau_{Ap}\to t$, $\chi\tau_{Ap}/a^2\to\hat{\chi}$, $\mu\tau_{Ap}/a^2\to\hat{\mu}$, $\tau_{Ap}/\mu_0\sigma a^2\to 1/\delta$, $\lambda\tau_{Ap}/\mu_0 a^4\to\hat{\lambda}$, $\tau_{Ap}\equiv Rq/v_A$, $\gamma\tau_{Ap}\to\hat{\gamma}$.] All the cross field transport coefficients are driven by the fluctuations, and the expressions are discussed in Ref.[10,30,42].

If the transport coefficients increase substantially, the stabilizing effects of $\hat{\chi}$ and $\hat{\mu}$ overcome the destabilizing effect of $\lambda$. The stability boundary is derived .

$$\alpha^{3/2}\lambda = f(s)\sqrt{\mu}\chi^{3/2} \tag{27}$$

where $f(s) \simeq \sqrt{6}s$ or 1.7 ($s \to 0$). This state is thermodynamically stable: the excess growth of the mode and enhanced transport coefficients lead to mode damping. When the mode amplitude and the transport coefficients are below Eq.(27), the mode continues growing.

From Eq.(27) we express $\chi$ in terms of the Prandtl numbers $\mu/\chi$ and $\lambda/\chi$ (note that $\lambda$ is proportional to the electron viscosity in the plasma frame[51]) as $\chi = \alpha^{3/2}(\lambda/\chi)\sqrt{\chi/\mu}/f(s)$. The ratios $\lambda/\chi$ and $\mu/\chi$ are given to be constant. We have $\lambda/\chi \simeq \delta^2/a^2$ and $\mu/\chi \simeq 1$ for electrostatic perturbations[32]. The formula for $\chi$ is finally obtained in an explicit form as

$$\chi = f(s)^{-1}q^2(R\beta'/r)^{3/2}\delta^2 v_A/R. \tag{28}$$

The typical perpendicular wave-number of the most unstable mode satisfies $k_\perp\delta \simeq 1/\sqrt{\alpha}$. The typical correlation time of the mode is estimated to be $\tau_c = 1/\gamma$, $\gamma \simeq \sqrt{\alpha/6s}(v_A/qR)$.

This form of $\chi$ is consistent with the experimental results known for the L-mode. For instance, the point model argument of the energy balance, $\tau_E = a^2/\chi$ and $2\pi^2a^2Rn_eT = \tau_E P$, provides the scaling law

$$\tau_E = C\, a^{0.4}R^{1.2}I_p^{0.8}P^{-0.6}A^{0.5}f^{-0.4}(n_e\ell_p/\sqrt{A})^{0.6}, \tag{29}$$

where C is a numerical coefficient and $\ell_p$ is the gradient scale length (nT)/|∇(nT)|. This result is consistent with the L-mode scaling law, including the dependences on a, R, $I_p$, P, A (ion mass number) and internal inductance[52]. Detailed comparison is given in Ref.[50], and the future study in application of the data-analysis is required.

It is noted that the typical wavelength and correlation times of the mode are calculated. $k_\perp \rho_i$ is of the order of 0.1 or less ($\rho_i$ is the ion gyroradius.) It should be noted that, though the dimensional relation $k_\perp \propto [B]/[\sqrt{T}]$ holds, $k_\perp$ does not scale with the *local* gyroradius. The collisionless skin depth would be a more relevant length. The typical time-scale $\tau_c$ depends on the average temperature, not explicitly on $n_e$ and B.

## (3.3) Influence of Radial Electric Field on Fluctuations

The important role of radial electric is described in §2.3 in connection with the improved confinement of the H-mode. Theories have also predicted that the inhomogeneous radial electric reduces fluctuations in the H-mode [7,17], and the explanation of the reduced fluctuations after the transition has been studied. The theory on the reduction of the low frequency fluctuations [22,53-56] has been either the linear theory, or the nonlinear theory of the fluid turbulence. We here briefly describe the recent theories on the radial electric field effect on microscopic fluctuations.

The effect of the inhomogeneous radial electric field on kinetic interactions has been discussed by Timofeev [57], and it has been found that the Landau resonance can be caused by the inhomogeneous ExB drift motion. This model has been applied to the stability of Bumpy torus and mirrors and has succeeded in explaining the effect of the radial electric field on the low frequency instabilities [58-60]. These theoretical predictions have been confirmed by the experimental observations[61].

We explain the $E_r$ inhomogeneity effect by taking the example of the linear stability. In the linear theory, the growth rate $\gamma$ can be approximately given as

$$\gamma = \gamma_0 - \gamma_{LD} \tag{30}$$

in the case of $\gamma \ll \omega_r$, where $\gamma_0$ is the drive by electrons, $\gamma_{LD}$ is the Landau damping by ions and $\omega_r$ is the real frequency. The Landau damping term may be written as [60]

$$\gamma_{LD} = \frac{\sqrt{\pi/2}(1+T_i/T_e)}{(1+T_i/T_e-\Lambda_0)^3} \frac{{\omega_*}^2{\Lambda_0}^2}{|k_\parallel v_{Ti}|} \exp\left\{-\left[\frac{\omega_r}{\sqrt{2}k_\parallel v_{Ti}}\right]^2\right\} \tag{31}$$

with $\omega_r = \omega_*[\Lambda_0/(1+T_i/T_e-\Lambda_0)+\alpha_1]$ and

$$k_\parallel^2 \simeq k_\parallel^2 + (k_y \rho_i \alpha_0/\lambda_n)^2 \tag{32}$$

where $\Lambda_0 = I_0(b)e^{-b}$ with $b = k_y^2\rho_i^2$. Here $\alpha_{0,1}$ are defined as

$\alpha_0 \equiv -\lambda_n{}^2(e/T_i)(dE_r/dx)$ and $\alpha_1 \equiv (eE_r/T_i)(n/n')$, respectively. Parameter $\alpha_1$ indicates the Doppler shift, and $\alpha_0$ causes the important modification of the effective parallel wave number.

The stability boundary is estimated by balancing the growth by electrons and ion damping. For $T_e \simeq T_i$,

$$\frac{1}{2-\Lambda_0}\,\frac{-n}{\lambda_n n'}\,\frac{A^2}{|\alpha_0|}\exp(-A^2/\alpha_0{}^2) > \frac{1}{\sqrt{2\pi}}\,\frac{\gamma_0}{\omega_*} \tag{32}$$

is required for stability, where $A = (-\lambda_n n'/n)\Lambda_0/(1+T_i/T_e-\Lambda_0)$. (Eigen value $\lambda_n n'/n$ is determined by the nonlocal calculation.) Generally, we obtain two roots for $|\alpha|$ from Eq.(32). The drift instability can be suppressed in the regions of $|\alpha_0|>\alpha_c$

$$\alpha_c \simeq A[\ln(\sqrt{2\pi}\omega_*/\gamma_0)]^{-1/2}. \tag{33}$$

The gradient influences the mode amplitude in a similar ways. Nonlinear theories on the fluid turbulence have suggested a simple and useful criterion, which is given that stabilization is expected if [62,63]

$$|E_r' k_\theta/Bk_r| \sim \gamma_L \tag{34}$$

where $\gamma_L$ is the linear growth rate in the absence of $E_r'$. Since the logarithm in Eq.(33) has only weak dependence, Eqs.(33) and (34) give similar results. Recent progress has shown that the curvature of $E_r$ has more strong influence on the stability and saturation level, and an intensive study is underway[53,84].

The anomalous transport can be reduced in two ways. The anomalous transport coefficient D by drift wave instabilities has been estimated as $D = F\gamma k^{-2}$, where the form factor F is a numerical coefficient of order of unity[62,63]. The reduction of the growth rate by the enhanced Landau damping decreases the anomalous transport. Nonlinear studies has evaluated F, and F is reduced by the inhomogeneous radial electric field. One may write as $D = D_0(F/F_0)(\gamma k_\perp^{-2})/(\gamma k_\perp^{-2})_0$, where the suffix 0 denotes the value in the absence of the radial electric field inhomogeneity. The dominant contribution in $F/F_0$ is discussed in [56,62] and is obtained as $F/F_0 \simeq 1/\{1+(2eB\alpha_0/k_y{}^2\lambda_n{}^2T\,D)^2\}$. Combining the $\alpha_0$ dependence of the linear growth rate, we have an approximate formula of $D/D_0$ as

$$\frac{D}{D_0} \simeq \left[ 1 - \frac{\omega_*}{\gamma_0} \frac{\sqrt{2\pi}}{2 - \Lambda_0} \frac{A^2}{|\alpha_0|} \exp\left[ -\frac{A^2}{\alpha_0{}^2} \right] \right] \frac{1}{1+[2eB\alpha_0/k_y{}^2\lambda_n{}^2TD]^2} \qquad (35)$$

The terms in round bracket come from the linear contribution. The effect of the parameter $\alpha_0$ on the linear growth rate causes a sharp reduction of the transport coefficient when the parameter $\alpha_0$ approaches to $\alpha_c$, the critical value for the stabilization.

It is also discussed that the microscopic fluctuation can generates the shear flow. The quasilinear contribution of the fluctuations on the radial electric field is discussed in §2.2. The other non-linear processes, such as the inverse cascade of the fluctuations, can also generate the shear flow[64-66].

## §4. Summary

In this article, we surveyed the on-going theoretical researches on the plasma confinement, illustrating the roles of the electric fields on the toroidal plasma confinement. The effect on the confinement can be generated either by the static electric field itself, through the introduction of the new thermodynamical force, or by the fluctuations. The influence is wide in variety of the observed phenomena and of the physics mechanism. The present pictures in the confinement theory extend further and wider than those presented here. The examples in this article would be illustrative how strong is the impact of the electric field in the magnetic confinement. (If one also reviews its influence on the impurity behaviour, the impact is evaluated to be stronger.) In summarizing this survey, Fig. 7 illustrate the mutual relation between the electric field and confinement. The research in this direction requires future continued efforts.

Based on these present progresses, the comprehensive study which unifies theories on the static electric field structure and on the fluctuations will make a considerable progress in the near future. In promoting such studies, the theories are not only improved through the test with experimental observations but also inspired by inspecting experimental observations. The experiments using the methed of the heavy ion beam probes have contributed significantly and uniquely to test these thinking quantitatively, or to create these modern plasma physics. Thus the establishment and elaboration of the heavy ion beam probes have been inevitable to the progress of the plasma physics in the fusion research.

## Acknowledgements

The authors would like to acknowledge discussion and collaboration with Drs. M. Azumi, K. Ida, H. Iguchi, H. Maeda, Y. Miura, T. Ohkawa, K. C. Shaing, S. Tsuji, F. Wagner, M. Wakatani, M. Yagi, S. Yoshikawa and H. Zushi. They are also grateful to discussions on the experimental data with the members of *ASDEX* team, JFT-2M group, D-III D group, JET Team, CHS and JIPP-TIIU group. This work is partly supported by the Grant-in-Aid for Scientific Research of the Ministry of Education of Japan.

## References

[1] B. B. Kadomtsev : *Plasma Turbulence*, ( Academic Press, London-New York, 1965 ).

[2] G. I. Budker: in *Plasma Physics and Problem of Controlled Thermonuclear Reactions*, Vol.1, Pergamon Press, New York (1961) 78.

[3] F. W. Baity, L. A. Berry, L. Bighel, et al.:in *Plasma Physics and Controlled Nuclear Fusion Research 1982*, Proc. 9th Int. Conf. Baltimore, 1982 (IAEA Vienna 1983) Vol.2, p185,

F. M. Bieniosek, K. A. Connor: Phys. Fluids **26** (1983) **2256**,

H. Ikegami, M. Hosokawa, H. Iguchi, et al.: in *Plasma Physics and Controlled Nuclear Fusion Research 1986*, Proc. 11th Int. Conf. Kyoto, 1986 (IAEA Vienna 1987) Vol.2, p489.

[4] L. M. Kovrizhnykh: Nucl. Fusion **24** (1984) 435.

[5] D. E. Hastings, W. A. Houlberg and K. C. Shaing: Nucl. Fusion **25** (1985) 445.

[6] H. Wobig, H. Maassberg, H. Renner, The WVII-A Team: in *Plasma Physics and Controlled Nuclear Fusion Research 1986*, Proc. 11th Int. Conf. Kyoto, 1986 (IAEA Vienna 1987) Vol.2, p369.

[7] S.-I. Itoh and K. Itoh : Phys. Rev. Lett. **60** (1988) 2276,

S.-I. Itoh and K. Itoh : Nucl . Fusion **29** (1989) 1031.

[8] J. Groebner, K. H. Burrel and R. P. Seraydarian: Phys. Rev. Lett. **64** (1990) 3015.

[9] K. Ida, S. Hidekuma, Y. Miura, et al: Phys. Rev. Lett. **65**

(1990) 1364.

Y. Miura, and JFT-2M Group : in *Plasma Physics and Controlled Nuclear Fusion Research 1990*, Proc. 13th Int. Conf. Washington, 1990, (IAEA, Vienna, 1991) Vol.1, p325.

[10] P. C. Leiwer : Nucl Fusion **25** (1985) 543 ; R. R. Domingeuz and R. E. Waltz : Nucl Fusion **67** (1987) 65.

[11] A. B. Mikhailovskii : *Theory of Plasma Instabilities*, ( Consultant Bureau, New York-London, 1974 ) Vol.1 and 2.

[12] B. B. Kadomtsev, O. P. Pogutse: in *Review of Plasma Physics* (ed. M. A. Leontovich, Consultants Bureau, New York, 1970) Vol.5, p249.

[13] A. J. Wootton, et al: Phys. Fluids B2 (1990) 2879.

[14] Experimental result using the HIBP method can be seen, e.g., in F. C. Jobes, R. L. Hickok: Nucl. Fusion **10** (1970) 195, G. A. Hallock, et al.: Phys. Rev. Lett. **56** (1986) 1248, R. L. Hickok, et al.: in *Plasma Physics and Controlled Nuclear Fusion Research 1990* (IAEA, Vienna, 1991) Vol.1, p.229, and D. W. Ross, et al.: Phys. Fluids **B3** (1991) 2251.

[15] A. A. Ware: Phys. Rev. Lett. **25** (1970) 15.

[16] *Physics of the Plasma-Wall Interactions in Controlled Fusion* (ed. D. E. Post and R. Behrisch), NATO ASI Series B131, (Prenum Press, New York, 1984).

[17] K. C. Shaing, E. C. Crume: Phys. Rev. lett. **63** (1989) 2369.

[18] R. D. Hazeltine: in Bull. Am. Phys. Soc. **33** (1988) 2107.

[19] K. Itoh, H. Sanuki, S.-I. Itoh: Nucl. Fusion **32** (1992) 1047.

[20] K. Itoh, H. Sanuki, J. Todoroki, et al.: Phys. Fluids **B3**

(1991) 1294.

[21] S. Yoshikawa, R. Freeman, M. Okabayashi: Research Report MATT-706 (Princeton Univ., 1969),
T. Ohkawa and F. L. Hinton: in ***Plasma Physics and Controlled Nuclear Fusion Research 1986***, Proc. 11th Int. Conf. Kyoto, 1986 (IAEA, Vienna, 1987) Vol.2, p221.

[22] S.-I. Itoh, K. Itoh, T. Ohkawa and N. Ueda : in ***Plasma Physics and Controlled Nuclear Fusion Research 1988***, Proc. 12th Int. Conf. Nice, 1988 (IAEA, Vienna, 1989) Vol.2, p23.
K. C. Shaing, G. S. Lee, B. Carreras, W. A. Houlberg and E. C. Crume : in ***Plasma Physics and Controlled Nuclear Fusion Research 1988***, Proc. 12th Int. Conf. Nice, 1988 (IAEA, Vienna, 1989) Vol.2, p13.

[23] T. H. Stix: Phys. Fluids **16** (1973) 1260.

[24] K. Ida, H. Yamada, H. Iguchi, et al.: Phys. Fluids **B3** (1991) 515.
H. Sanuki, K. Itoh, K. Ida, S.-I. Itoh: J. Phys. Soc. Jpn. **60** (1991) 3698.

[25] F. Wagner, G. Becker, K. Behringer et al : Phys. Rev. Lett. **49** (1982) 1408.

[26] ASDEX Team: Nuclear Fusion **29** (1989) 1959.

[27] F. X. Soeldner, et al.: Phys. Rev. Lett. 61, 1105 (1988).

[28] J. D. Strachan, et al.: Phys. Rev. Lett. 58, 1004 (1987).

[29] S. I. Itoh: J. Phys. Soc. Jpn. **59** (1990) 3431.

[30] S. Tange, S. Inoue, K. Itoh, K. Nishikawa: J. Phys. Soc. Jpn. **46** (1979) 266.

[31] R. D. Hazeltine, S. M. Mahajan, D. A. Hichcock: Phys. Fluids

**24** (1981) 1164.

[32] S.-I. Itoh: Phys. Fluids **B4** (1992) 796.

[33] L. D. Landau, E. M. Lifshitz: Fluid Mechanics ( Pergamon Press, London, 1959) (Transl. J. B. Sykes, W. H. Reid) 208.

[34] K. Itoh, S.-I. Itoh: Research Report NIFS-158 (1992), Nucl. Fusion **32** (1992) in press.

[35] R. J. Taylor, M. L. Brown, B. D. Fried, et al.: Phys. Rev. Lett. **63** (1989) 2365.

[36] R. R. Waynants, et al.: in ***Plasma Physics and Controlled Nuclear Fusion Research 1990*** (IAEA, Vienna, 1991) Vol.1, p.473.

[37] S. Tsuji, K. Ushigusa, Y. Ikeda, et al.: Phys. Rev. Lett. **64** (1990) 1023.
S. Tsuji, S. Ide, M. Seki, et al.:in ***Plasma Physics and Controlled Nuclear Fusion Research 1990*** (IAEA, Vienna, 1991) Vol.1, p.659.

[38] H. Zohm, et al.: Nucl. Fusion **32** (1992) 489.

[39] J. W. Connor, et al.: Proc. Royal Soc. London **A365** (1979) 1.
H. R. Strauss: Phys. Fluids **24** (1981) 2004, and
A. Sykes, et al.: Plasma Phys. Contr. Fusion **29** (1987) 719.

[40] S.-I. Itoh, et al.: Phys. Rev. Lett. **67** (1991) 2485,
S.-I. Itoh, et al.: in Proc. 14th Int. Conf. on Plasma Physics and Controlled Nuclear Fusion Research, Wurzburg, 1992, paper IAEA-CN-56/D-4-19.
See also E. Yahagi, K. Itoh, M. Wakatani, Plasma Physics and Controlled Fusion **30** (1988) 1009 for the effect of the shear viscosity.

[41] J. Neuhauser, et al.: Nucl. Fusion **26** (1986) 1679.
[42] W. Horton: in ***Handbook of Plasma Physics*** (ed. M. N. Rosenbluth and R. E. Sagdeev, *Elsevier Science* Publishers B. V., *1984*) *Vol.2,* §6.4.
[43] See *for instance* P. H. Diamond, et al.: in ***Plasma Physics and Controlled Nuclear Fusion Research 1990*** (IAEA, Vienna, 1991) Vol.2, 9.
[44] K. C. Shaing: Phys. Fluids **31** 2249 (1988).
[45] R. J. Goldston: Plasma Phys. Control. Fusion **26** (1984) 87.
[46] P. Yushmanov, et al.: Nucl. Fusion **30** (1990) 1999.
[47] T. Ohkawa: Phys. Letters **67A** (1978) 35.
[48] S. P. Hirshman, K. Molvig: Phys. Rev. Lett. **42** (1979) 648.
[49] K. Itoh, S.-I. Itoh, A. Fukuyama: Phys. Rev. Lett. **69** (1992) 1050.
[50] K. Itoh, S.-I. Itoh, A. Fukuyama, M. Yagi, M. Azumi: in Proc. 14th Int. Conf. on Plasma Physics and Controlled Nuclear Fusion Research, Wurzburg, 1992, paper IAEA-CN-56/H-2-2, and 'L-mode Confinement Model Based on Transport-MHD Theory in Tokamaks' Research Report NIFS 192 (NIFS, 1992).
[51] J. Schmidt, S. Yoshikawa: Phys. Rev. Lett. **26** (1971) 753. See also A. J. Lichtenberg, K. Itoh, S.-I. Itoh, A. Fukuyama: Nucl. Fusion **31** (1992) 495.
[52] M. C. Zarnstorff, et al.: in ***Plasma Physics and Controlled Nuclear Fusion Research 1990*** (IAEA, Vienna, 1991) Vol.1, 109.
[53] S. Inoue, K. Itoh, S. Yoshikawa: J. Phys. Soc. Jpn. **49** (1980) 367.
[54] S.-I. Itoh, H. Sanuki, K. Itoh: J. Phys. Soc. Jpn. **60** (1991)

2505.

[55] H. Sugama, M. Wakatani: J. Phys. Soc. Jpn. **58** (1989) 3859.
H. Sugama, M. Wakatani: *Phys. Fluids* ***B3*** *(1991) 1110.*

[56] H. Bigrali, P. H. Diamond and P. W. Terry: Phys. Fluids **B2** (1989) 1.

[57] A. V. Timofeev: Sov. Phys. Tech. Phys. **10** (1967) 1331 and Plasma Physics **10** (1968) 235.

[58] H. Sanuki: J. Phys. Soc. Japan **52** (1983) 511 ;

[59] H. Sanuki and R. D. Ferraro: Physica Scripta **34** (1986) 58.

[60] H. Sanuki: Phys. Fluids **27** (1984) 2500.

[61] A. Mase, et al.: *Phys. Rev. Lett.* ***64*** *(1990) 2281.*

[62] K. C. Shaing: Comments on Plasma Phys. Cont. Fusion **14** (1991) 41.

[63] A. B. Hassam: Comments on Plasma Phys. Cont. Fusion **14** (1991) 275.

[64] P. H. Diamond, et al. in Proc. 14th Int. Conf. on Plasma Physics and Controlled Nuclear Fusion Research, Wurzburg, 1992, paper IAEA-CN-56/D-2-4.
L. Garcia, et al., ibid. paper IAEA-CN-56/D-4-6.

[65] A. Hasegawa, M. Wakatani: Phys. Rev. Lett. **59** (1987) 1581.
M. Wakatani, et al.: Phys. Fluids **B4** (1992) 1754.

[66] J. Drake, et al.: in Proc. 14th Int. Conf. on Plasma Physics and Controlled Nuclear Fusion Research, Wurzburg, 1992, paper IAEA-CN-56/D-2-5.

**Figure Captions**

Fig.1 Radial electric field profiles are plotted for the high density case of CHS plasma (a). Loss cone boundary for the particle of $W_b$=18keV is shown in (b). For the experimental parameters, see Ref.[24].

Fig. 2 (a) Density profile for various values of $\sqrt{\nu_a/\nu_\mu}$ (from 0.1 to 10) for fixed value of $A_0$. ($A_0=a/\lambda_n-C_1-a^2\langle S\rangle/D_e$; increment of $A_0$ denotes the reduction of the edge neutral density.) (a), and flow velocity ( normalized to $v_{Ti}\rho_p/a$ ) (b) Radial profile of the static potential corresponding to the shear flow. (c) Density profile for various values of $A_0$ (3, 5, 10, 20) for the fixed values of $\nu_a/\nu_\mu$(=1).

Fig.3 Schematic model relation of the gradient ($\nabla n$, $\nabla T$) and flux ($\Gamma$, q) for the edge plasma, in order to explain the rapid change of the energy loss at the onset of H-mode transition.

Fig.4 Balance of loss cone loss $\Gamma_i^{orbit}$ and electron loss $\Gamma_e$ determines the radial electric field $X=e\rho_p E_r/T_i$ (a). For the case of A (small $\lambda=\rho_p n'/n$), one large-flux solution is allowed. Multiple solutions are possible for the medium $\lambda$ case (B and C), and the one small-flux solution is allowed for large value of $\lambda$ (D). The resultant flux as a function of $\lambda$ is shown in (b). The characteristic response in Fig.4 is recovered. When the electron loss term $\Gamma_e$ is negligible, the ion viscosity-driven flux $-\Gamma_i^{NC(s)}$ and $\Gamma_i^{orbit}$ (solid and dashed lines, respectively) determine the radial electric field (c). The function $\Gamma(\lambda)$ shows the similar response as in (b).

Fig.5 Model of the effective diffusivity D ($D=-\Gamma/\nabla n$) as a function of the gradient parameter $\lambda/\nu_i$ (a). Transition occurs at points A and B'. Two branches H and L are shown. The predicted oscillation, for given constant flux from core, is shown in (b). The profile of D at the two time slices (arrows in (b)) are shown (c). $x=0$ corresponds to the surface, and $x<-2$ to the core plasma.

Fig.6 Local coordinates for the inhomogeneous plasma.

Fig.7 Schematic diagram between the radial electric field/ rotation, the radial current, anomalous transport, and plasma fluxes.

Fig. 1

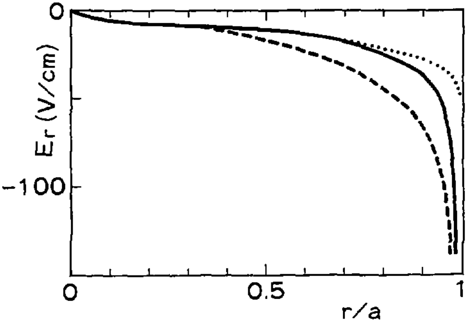


(a)

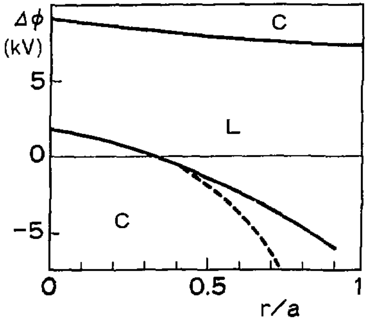


(b)

Fig. 2

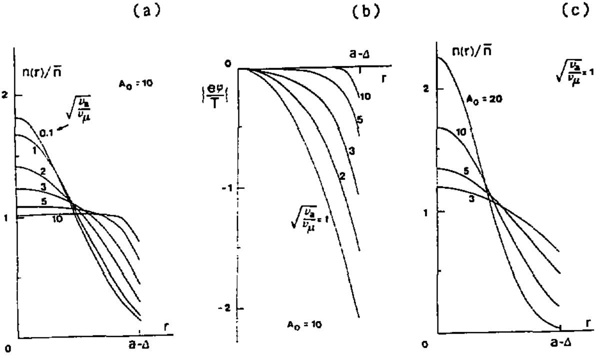
(a)
n(r)/n̄
A0 = 10
√(νa/νμ)
0.1
1
2
3
5
10
r
a-Δ
0
1
2
(b)
a-Δ
r
|eφ/T|
0
-1
-2
10
5
3
2
√(νa/νμ) = 1
A0 = 10
(c)
n(r)/n̄
√(νa/νμ) = 1
A0 = 20
10
5
3
r
a-Δ
0
1
2

Fig. 3

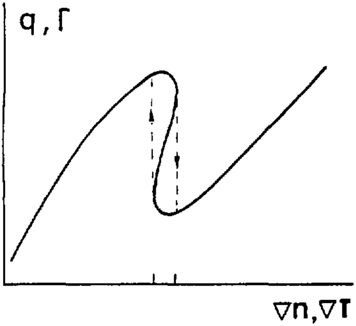

Fig. 4

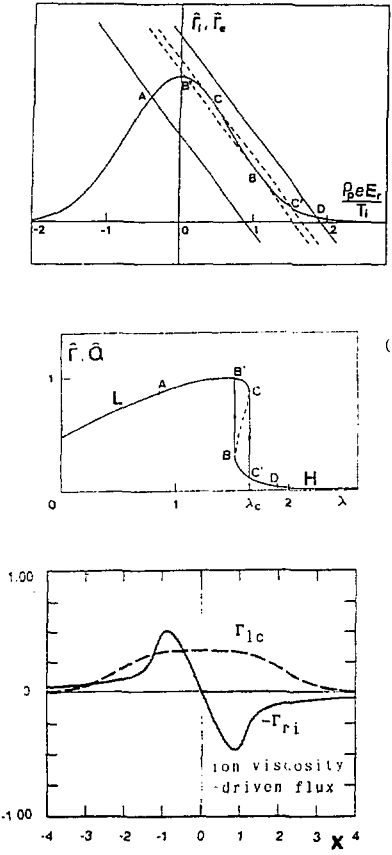

A
B'
C
B
C'
D
-2
-1
0
1
2
L
H
λc
λ
Γ1c
-Γri
ion viscosity
-driven flux
1.00
-1.00
-4
-3
-2
-1
0
1
2
3
4
X


(a)

(b)

( )

Fig. 5

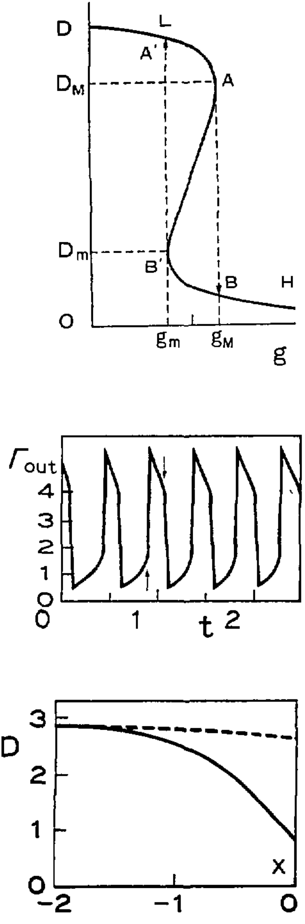


(a)

(b)

(c)

Fig. 6

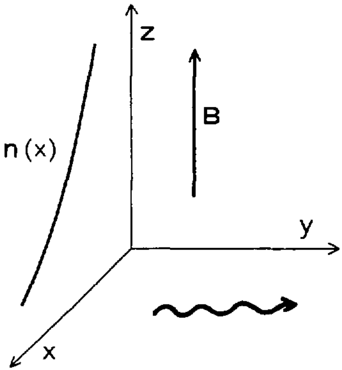

Fig.7

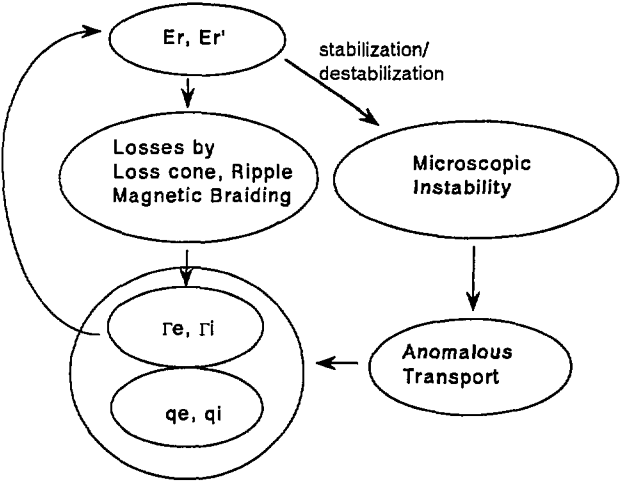

Er, Er'
stabilization/
destabilization
Losses by
Loss cone, Ripple
Magnetic Braiding
Microscopic
Instability
Γe, Γi
qe, qi
Anomalous
Transport

## Recent Issues of NIFS Series

NIFS-160 H. Sanuki, K. Itoh and S.-I. Itoh, *Effects of Nonclassical Ion Losses on Radial Electric Field in CHS Torsatron/Heliotron*; July 1992

NIFS-161 O. Motojima, K. Akaishi, K. Fujii, S. Fujiwaka, S. Imagawa, H. Ji, H. Kaneko, S. Kitagawa, Y. Kubota, K. Matsuoka, T. Mito, S. Morimoto, A. Nishimura, K. Nishimura, N. Noda, I. Ohtake, N. Ohyabu, S. Okamura, A. Sagara, M. Sakamoto, S. Satoh, T. Satow, K. Takahata, H. Tamura, S. Tanahashi, T. Tsuzuki, S. Yamada, H. Yamada, K. Yamazaki, N. Yanagi, H. Yonezu, J. Yamamoto, M. Fujiwara and A. Iiyoshi, *Physics and Engineering Design Studies on Large Helical Device*; Aug. 1992

NIFS-162 V. D. Pustovitov, *Refined Theory of Diamagnetic Effect in Stellarators;* Aug. 1992

NIFS-163 K. Itoh, *A Review on Application of MHD Theory to Plasma Boundary Problems in Tokamaks*; Aug. 1992

NIFS-164 Y.Kondoh and T.Sato, *Thought Analysis on Self-Organization Theories of MHD Plasma*; Aug. 1992

NIFS-165 T. Seki, R. Kumazawa, T. Watari, M. Ono, Y. Yasaka, F. Shimpo, A. Ando, O. Kaneko, Y. Oka, K. Adati, R. Akiyama, Y. Hamada, S. Hidekuma, S. Hirokura, K. Ida, A. Karita, K. Kawahata, Y. Kawasumi, Y. Kitoh, T. Kohmoto, M. Kojima, K. Masai, S. Morita, K. Narihara, Y. Ogawa, K. Ohkubo, S. Okajima, T. Ozaki, M. Sakamoto, M. Sasao, K. Sato, K. N. Sato, H. Takahashi, Y. Taniguchi, K. Toi and T. Tsuzuki, *High Frequency Ion Bernstein Wave Heating Experiment on JIPP T-IIU Tokamak*; Aug. 1992

NIFS-166 Vo Hong Anh and Nguyen Tien Dung, *A Synergetic Treatment of the Vortices Behaviour of a Plasma with Viscosity*; Sep. 1992

NIFS-167 K. Watanabe and T. Sato, *A Triggering Mechanism of Fast Crash in Sawtooth Oscillation*; Sep. 1992

NIFS-168 T. Hayashi, T. Sato, W. Lotz, P. Merkel, J. Nührenberg, U. Schwenn and E. Strumberger, *3D MHD Study of Helias and Heliotron;* Sep. 1992

NIFS-169 N. Nakajima, K. Ichiguchi, K. Watanabe, H. Sugama, M. Okamoto, M. Wakatani, Y. Nakamura and C. Z. Cheng, *Neoclassical Current and Related MHD Stability, Gap Modes, and Radial Electric Field Effects in Heliotron and Torsatron Plasmas;* Sep. 1992

NIFS-170 H. Sugama, M. Okamoto and M. Wakatani, *$K$-$\varepsilon$ Model of Anomalous*

*Transport in Resistive Interchange Turbulence* ; Sep. 1992

NIFS-171 H. Sugama, M. Okamoto and M. Wakatani, *Vlasov Equation in the Stochastic Magnetic Field* ; Sep. 1992

NIFS-172 N. Nakajima, M. Okamoto and M. Fujiwara, *Physical Mechanism of $E_\varphi$-Driven Current in Asymmetric Toroidal Systems* ; Sep.1992

NIFS-173 N. Nakajima, J. Todoroki and M. Okamoto, *On Relation between Hamada and Boozer Magnetic Coordinate System* ; Sep. 1992

NIFS-174 K. Ichiguchi, N. Nakajima, M. Okamoto, Y. Nakamura and M. Wakatani, *Effects of Net Toroidal Current on Mercier Criterion in the Large Helical Device* ; Sep. 1992

NIFS-175 S. -I. Itoh, K. Itoh and A. Fukuyama, *Modelling of ELMs and Dynamic Responses of the H-Mode* ; Sep. 1992

NIFS-176 K. Itoh, S.-I. Itoh, A. Fukuyama, H. Sanuki, K. Ichiguchi and J. Todoroki, *Improved Models of $\beta$-Limit, Anomalous Transport and Radial Electric Field with Loss Cone Loss in Heliotron / Torsatron* ; Sep. 1992

NIFS-177 N. Ohyabu, K. Yamazaki, I. Katanuma, H. Ji, T. Watanabe, K. Watanabe, H. Akao, K. Akaishi, T. Ono, H. Kaneko, T. Kawamura, Y. Kubota, N. Noda, A. Sagara, O. Motojima, M. Fujiwara and A. Iiyoshi, *Design Study of LHD Helical Divertor and High Temperature Divertor Plasma Operation* ; Sep. 1992

NIFS-178 H. Sanuki, K. Itoh and S.-I. Itoh, *Selfconsistent Analysis of Radial Electric Field and Fast Ion Losses in CHS Torsatron / Heliotron* ; Sep. 1992

NIFS-179 K. Toi, S. Morita, K. Kawahata, K. Ida, T. Watari, R. Kumazawa, A. Ando, Y. Oka, K. Ohkubo, Y. Hamada, K. Adati, R. Akiyama, S. Hidekuma, S. Hirokura, O. Kaneko, T. Kawamoto, Y. Kawasumi, M. Kojima, T. Kuroda, K. Masai, K. Narihara, Y. Ogawa, S. Okajima, M. Sakamoto, M. Sasao, K. Sato, K. N. Sato, T. Seki, F. Shimpo, S. Tanahashi, Y. Taniguchi, T. Tsuzuki, *New Features of L-H Transition in Limiter H-Modes of JIPP T-IIU* ; Sep. 1992

NIFS-180 H. Momota, Y. Tomita, A. Ishida, Y. Kohzaki, M. Ohnishi, S. Ohi, Y. Nakao and M. Nishikawa, *$D$-$^3He$ Fueled FRC Reactor "Artemis-L"* ; Sep. 1992

NIFS-181 T. Watari, R. Kumazawa, T. Seki, Y. Yasaka, A. Ando, Y. Oka, O. Kaneko, K. Adati, R. Akiyama, Y. Hamada, S. Hidekuma, S. Hirokura, K. Ida, K. Kawahata, T. Kawamoto, Y. Kawasumi,

S. Kitagawa, M. Kojima, T. Kuroda, K. Masai, S. Morita, K. Narihara, Y. Ogawa, K. Ohkubo, S. Okajima, T. Ozaki, M. Sakamoto, M. Sasao, K. Sato, K. N. Sato, F. Shimpo, H. Takahashi, S. Tanahasi, Y. Taniguchi, K. Toi, T. Tsuzuki and M. Ono, *The New Features of Ion Bernstein Wave Heating in JIPP T-IIU Tokamak*; Sep, 1992

NIFS-182 K. Itoh, H. Sanuki and S.-I. Itoh, *Effect of Alpha Particles on Radial Electric Field Structure in Torsatron / Heliotron Reactor*; Sep. 1992

NIFS-183 S. Morimoto, M. Sato, H. Yamada, H. Ji, S. Okamura, S. Kubo, O. Motojima, M. Murakami, T. C. Jernigan, T. S. Bigelow, A. C. England, R. S. Isler, J. F. Lyon, C. H. Ma, D. A. Rasmussen, C. R. Schaich, J. B. Wilgen and J. L. Yarber, *Long Pulse Discharges Sustained by Second Harmonic Electron Cyclotron Heating Using a 35GHz Gyrotron in the Advanced Toroidal Facility*; Sep. 1992

NIFS-184 S. Okamura, K. Hanatani, K. Nishimura, R. Akiyama, T. Amano, H. Arimoto, M. Fujiwara, M. Hosokawa, K. Ida, H. Idei, H. Iguchi, O. Kaneko, T. Kawamoto, S. Kubo, R. Kumazawa, K. Matsuoka, S. Morita, O. Motojima, T. Mutoh, N. Nakajima, N. Noda, M. Okamoto, T. Ozaki, A. Sagara, S. Sakakibara, H. Sanuki, T. Saki, T. Shoji, F. Shimbo, C. Takahashi, Y. Takeiri, Y. Takita, K. Toi, K. Tsumori, M. Ueda, T. Watari, H. Yamada and I. Yamada, *Heating Experiments Using Neutral Beams with Variable Injection Angle and ICRF Waves in CHS*; Sep. 1992

NIFS-185 H. Yamada, S. Morita, K. Ida, S. Okamura, H. Iguchi, S. Sakakibara, K. Nishimura, R. Akiyama, H. Arimoto, M. Fujiwara, K. Hanatani, S. P. Hirshman, K. Ichiguchi, H. Idei, O. Kaneko, T. Kawamoto, S. Kubo, D. K. Lee, K. Matsuoka, O, Motojima, T. Ozaki, V. D. Pustovitov, A. Sagara, H. Sanuki, T. Shoji, C. Takahashi, Y. Takeiri, Y. Takita, S. Tanahashi, J. Todoroki, K. Toi, K. Tsumori, M. Ueda and I. Yamada, *MHD and Confinement Characteristics in the High-$\beta$ Regime on the CHS Low-Aspect-Ratio Heliotron / Torsatron*; Sep. 1992

NIFS-186 S. Morita, H. Yamada, H. Iguchi, K. Adati, R. Akiyama, H. Arimoto, M. Fujiwara, Y. Hamada, K. Ida, H. Idei, O. Kaneko, K. Kawahata, T. Kawamoto, S. Kubo, R. Kumazawa, K. Matsuoka, T. Morisaki, K. Nishimura, S. Okamura, T. Ozaki, T. Seki, M. Sakurai, S. Sakakibara, A. Sagara, C. Takahashi, Y. Takeiri, H. Takenaga, Y. Takita, K. Toi, K. Tsumori, K. Uchino, M. Ueda, T. Watari, I. Yamada, *A Role of Neutral Hydrogen in CHS Plasmas with Reheat and Collapse and Comparison with JIPP T-IIU Tokamak Plasmas*; Sep. 1992

NIFS-187 K. Ioth, S.-I. Itoh, A. Fukuyama, M. Yagi and M. Azumi, *Model of the L-Mode Confinement in Tokamaks*; Sep. 1992

NIFS-188 K. Itoh, A. Fukuyama and S.-I. Itoh, *Beta-Limiting Phenomena in High-Aspect-Ratio Toroidal Helical Plasmas*; Oct. 1992

NIFS-189 K. Itoh, S. -I. Itoh and A. Fukuyama, *Cross Field Ion Motion at Sawtooth Crash* ; Oct. 1992

NIFS-190 N. Noda, Y. Kubota, A. Sagara, N. Ohyabu, K. Akaishi, H. Ji, O. Motojima, M. Hashiba, I. Fujita, T. Hino, T. Yamashina, T. Matsuda, T. Sogabe, T. Matsumoto, K. Kuroda, S. Yamazaki, H. Ise, J. Adachi and T. Suzuki, *Design Study on Divertor Plates of Large Helical Device (LHD)* ; Oct. 1992

NIFS-191 Y. Kondoh, Y. Hosaka and K. Ishii, *Kernel Optimum Nearly-Analytical Discretization (KOND) Algorithm Applied to Parabolic and Hyperbolic Equations* : Oct. 1992

NIFS-192 K. Itoh, M. Yagi, S.-I. Itoh, A. Fukuyama and M. Azumi, *L-Mode Confinement Model Based on Transport-MHD Theory in Tokamaks* ; Oct. 1992

NIFS-193 T. Watari, *Review of Japanese Results on Heating and Current Drive* ; Oct. 1992

NIFS-194 Y. Kondoh, *Eigenfunction for Dissipative Dynamics Operator and Attractor of Dissipative Structure* ; Oct. 1992

NIFS-195 T. Watanabe, H. Oya, K. Watanabe and T. Sato, *Comprehensive Simulation Study on Local and Global Development of Auroral Arcs and Field-Aligned Potentials* ; Oct. 1992

NIFS-196 T. Mori, K. Akaishi, Y. Kubota, O. Motojima, M. Mushiaki, Y. Funato and Y. Hanaoka, *Pumping Experiment of Water on B and* $LaB_6$ *Films with Electron Beam Evaporator* ; Oct., 1992

NIFS-197 T. Kato and K. Masai, *X-ray Spectra from Hinotori Satellite and Suprathermal Electrons* ; Oct. 1992

NIFS-198 K. Toi, S. Okamura, H. Iguchi, H. Yamada, S. Morita, S. Sakakibara, K. Ida, K. Nishimura, K. Matsuoka, R. Akiyama, H. Arimoto, M. Fujiwara, M. Hosokawa, H. Idei, O. Kaneko, S. Kubo, A. Sagara, C. Takahashi, Y. Takeiri, Y. Takita, K. Tsumori, I. Yamada and H. Zushi, *Formation of H-mode Like Transport Barrier in the CHS Heliotron / Torsatron* ; Oct. 1992

NIFS-199 M. Tanaka, *A Kinetic Simulation of Low-Frequency Electromagnetic Phenomena in Inhomogeneous Plasmas of Three-Dimensions* ; Nov. 1992